

# A robust and self-powered tilt sensor based on annular liquid-solid interfacing triboelectric nanogenerator for ship attitude sensing



Song Wang<sup>a,1</sup>, Yan Wang<sup>a,1</sup>, Dehua Liu<sup>a</sup>, Ziyi Zhang<sup>a</sup>, Wenxiang Li<sup>a</sup>, Changxin Liu<sup>a</sup>, Taili Du<sup>a</sup>, Xiu Xiao<sup>a</sup>, Liguang Song<sup>a</sup>, Hongchen Pang<sup>b</sup>, Minyi Xu<sup>a,\*</sup>

<sup>a</sup> Marine Engineering College, Dalian Maritime University, Dalian, 116026, China

<sup>b</sup> School of Mechanical and Power Engineering, Guangdong Ocean University, Zhanjiang, 524088, China

## ARTICLE INFO

### Article history:

Received 18 August 2020

Received in revised form 5 November 2020

Accepted 20 November 2020

Available online 24 November 2020

### Keywords:

Tilt sensor

Triboelectric nanogenerator

Self-powered sensor

Smart ship

## ABSTRACT

Ship's attitude information is of great significance for navigation safety, cargo handling monitoring, and operation management. It is highly desired to develop an electromechanical integrated tilt sensor which can work well under harsh environment. In this paper, a robust and self-powered tilt sensor based on annular liquid-solid interfacing triboelectric nanogenerator (TENG) is to be proposed and systematically investigated. The TENG tilt sensor is composed of an annular polytetrafluoroethylene (PTFE) tube with copper electrodes segment disposed on the surface and the internal liquid which is encapsulated in PTFE tube with no air bubble. Studies on electrode width and liquid type are conducted to reasonably design the TENG sensor structure and improve its sensitivity. By conducting the durability test, the TENG tilt sensor demonstrates stable output performance and high sensitivity characteristics in low-frequency and low-amplitude inclination conditions. Moreover, the TENG tilt sensor hardly fails due to parts wear since there are no moving parts in it. The advantage of durability, maintenance-free, and independent with the external environment are highlighted in a harsh environment with high humidity, high salinity and strong magnetic field. Therefore, the present TENG tilt sensor is of practical significance for improving the automation and intelligence of ships.

© 2020 Elsevier B.V. All rights reserved.

## 1. Introduction

It is of great significance for navigation safety, cargo handling monitoring, and operation management by acquiring information about the shipping conditions through sensor networks and information sensing technology [1]. With the development of smart ships, information sensing technology based on wireless sensor networks has become an important way to achieve the above functions. Large ocean-going vessels sailing in the ocean are always swaying due to environmental factors such as wind wave and ocean current, especially in rough sea conditions. Rough sea condition poses a significant safety hazard to the ship's operations [2]. The U.S. Navy lists the tilt limit and sway frequency of ships in extremely rough sea conditions in the ship motion and attitude standards, i.e.  $\pm 45^\circ$  and 0.07~0.33 Hz [3]. If the ship's movement posture can be measured accurately, it must be of great significance to the safe

navigation of ships, anti-rolling control, etc. [4]. Therefore, it is important to obtain and save the ship's attitude information in time.

Traditional tilt sensors are divided into mechanical sensors and electronic sensors. Mechanical sensors are stable and low cost, such as vertical gravitational pendulum sensors, horizontal gravitational pendulum sensors. These sensors are usually used to detect the tilt of a ship against a horizontal and vertical plan. Angle change is obtained by manual observation of the instrument pointer, and there are no electronic signals for indicating or alarming. Electronic sensors have good sensitivity, but it can be affected by harsh conditions such as high temperature, high pressure and magnetic fields inside the ship [5–8]. Mechanical and electronic sensors are independent of each other, which not only complicates the maintenance process but also greatly increases the fabrication cost. The maintenance work requires high professionalism for personnel, and crews generally do not have this ability. Therefore, sensors with simple structures and maintenance-free are more suitable for such occasions. There still lacks of an electromechanical integrated tilt sensor with high reliability and long service life. Therefore, a robust tilt sensor and a sensing method are highly in demand as a ship attitude sensing system which performance is independent of external

\* Corresponding author.

E-mail address: [xuminyi@dlnmu.edu.cn](mailto:xuminyi@dlnmu.edu.cn) (M. Xu).

<sup>1</sup> S. Wang, Y. Wang and D. Liu contribute equally to this work.

environments and harsh sea conditions. It is necessary to research a sensor with high reliability and capable of providing electronic signals.

Recently, triboelectric nanogenerator (TENG) based on the coupling of triboelectrification effect and electrostatic induction has been developed for energy harvesting and sensing [9–17]. At present, several triboelectric nanogenerators based on the liquid-solid interfacing method in the contact and separation of the polymer material and the liquid have been proposed [18–22]. Lin et al. [23] studied the contact and separation of PTFE with water to produce electrical energy. TENG is not only a new energy harvesting technology but also a rich application in the field of self-powered sensing. Zhang et al. [24] studied the application of U-tube triboelectric nanogenerator in pressure and flow rate sensors. Pan et al. [25] studied the application of U-TENG in solution concentration sensing. Other various types of TENGs have been developed for self-powered sensors to detect the information of water wave, vibration, pressure, acceleration, displacement, humidity, pulse, gas flow, etc. [19,25–35].

In this paper, an annular liquid-solid interfacing triboelectric nanogenerator is proposed as a ship attitude monitoring device. It has the advantages of a more robust, self-powered, lower cost, and simpler manufacturing process compared to the previous ship tilt sensors. The influences of the electrode width and internal fluid type on the output characteristics of the TENG tilt sensor are systematically investigated in this work. Charge transfer mechanism, finite-element simulation of the potential distribution and output characteristics of the TENG tilt sensor are analyzed in theory. The tilt angle can be determined by the treated signal ( $dV_{OC}/dt$ ) of the TENG tilt sensor, and tilt direction can be reflected by the positive and negative of its peak value. The advantage of durability, maintenance-free, and independent with the external environment are highlighted in a harsh environment with high humidity, high salinity and strong magnetic field. By conducting the durability test, the TENG tilt sensor demonstrates stable output performance and high sensitivity characteristics in low-frequency and low-amplitude inclination conditions.

## 2. Device fabrication and experimental setup

### 2.1. Device fabrication

The TENG tilt sensor is applied to monitor the attitude of the ship as shown in Fig. 1a. The sensor is fixed on the horizontal platform of the ocean-going vessel, which moves with the rolling and pitching of the ship. The structure and principle of the TENG tilt sensor are shown in Fig. 1b. In the initial state, the sensor's symmetry line  $N_2$  is vertical. When the sensor is tilted, the angle formed between the symmetry line  $N_2$  and the vertical line  $N_1$  is defined as  $\alpha$ . The angle corresponding to the arc length of the liquid flowing in the tube is the same as the angle  $\alpha$ . By judging the arc length through which the internal liquid flows, the tilt angle  $\alpha$  can be calculated. Besides, the fabrication of the TENG tilt sensor is shown in Fig. 1c. The TENG tilt sensor is composed of a circular polytetrafluoroethylene (PTFE) tube with a copper metal electrodes segment disposed on the surface. The diameter of the circular PTFE tube, which is an outer diameter of 6 mm and an inner diameter of 5 mm. The 6 mm diameter of PTFE annular is chosen concerning the work of Pan et al. [25]. The large diameter of the annular had a relatively poor output performance because of the better fluidity, which will make it difficult for water to fill the cross-sectional area of the PTFE annular, and the free surface is formed that can make the electric signal unstable. A smaller electrode and larger diameter of the annular can result in the high resolution of the TENG tilt sensor.

According to the results of Niu et al. [36], the voltage  $V$  for the dielectric-to-dielectric sliding-mode TENG can be estimated by,

$$V = \sigma \omega v R \ln \left( \frac{l - vt}{l} \right) \quad (1)$$

here  $\sigma$  is the surface charge density,  $\omega$  is the inherent parameters of water that affect the output performance,  $l$  is the arc length of the blank.  $v$  is the velocity. As the frequency of the tilt sensor is set to 0.25 Hz, the large blank region and width of the electrode result in the high velocity and low voltage signal. In order to improve the resolution of the sensor and the convenience of processing, a 2 mm electrode and a 200 mm diameter of the PTFE annular are used to fabricate the TENG tilt sensor. The length of the blank tube region with the unattached electrode at the lower end of the tilt sensor is 12 mm. The internal fluid is encapsulated in a PTFE tube with no air bubble, the length of the internal fluid is 12 mm, as shown in Fig. 1c (ii). The presence of bubbles can result in discontinuity of the electric signals as the air bubbles cannot induce the charge transfer. The effective method to eliminate the air bubbles is to tilt the sensor at a certain angle when filling the liquid into the tube. The filling speed should be controlled, the injector and PTFE tube contacts together. The internal liquid maintains good fluidity in order to sense changes in tilt angle in real-time, and no bubbles in a low frequency as ship tilt frequency is low. The copper electrode is distributed symmetrically on the left and right along the PTFE tube, as shown in Fig. 1c (iii). Each copper electrode is connected to a wire. The left electrode wires are connected, and the same connecting method for the right wires, as shown in Fig. 1c (iv). It can be concluded that the TENG tilt sensor hardly fails due to parts wear since there are no moving parts in it.

### 2.2. Experiment setup

The experimental apparatus is shown in Fig. 2. The system consists of a swing test bench, TENG tilt sensor, electrometer and data acquisition (DAQ) board. The electrodes are connected to the electrometer (Keithley 6514) through copper wire. The electric signals are transferred to a data acquisition (DAQ) board (National Instruments, DAQ-9174) for acquisition. The open circuit voltage ( $V_{OC}$ ), short circuit current ( $I_{SC}$ ), and transferred charge ( $Q_{SC}$ ) signals are shown and saved in LabView<sup>®</sup> based computer. The computer is used to control the tilt angle of the swing table through a controller. The TENG tilt sensor is fixed on the base plate of the swing test bench as shown in Fig. 2.

## 3. Results and discussion

### 3.1. Working principle

A schematic diagram of the charge distribution of TENG tilt sensor is shown in Fig. 3a, which is similar to the liquid-solid freestanding TENG [9]. When the TENG tilt sensor is balanced in a horizontal position, there is no potential difference between the two-sided electrodes Fig. 3a (ii). The water flows down the right column and flows upward along the left column, the excess water on the left side carries a positive charge, repelling the positive charge of the copper electrode, thereby electron transfer is achieved in an external circuit to balance the polarization charge distribution caused by the motion of liquid, as shown in Fig. 3a (i). Subsequently, the reversed flowing of the water leads to a reversed transfer of electrons through the external circuit. The COMSOL Multiphysics software based on finite-element simulation is employed to calculate the potential distribution across the distributed electrodes at different states, as shown in Fig. 3b. The potential distribution is clearly displayed that the liquid column flows through the elec-

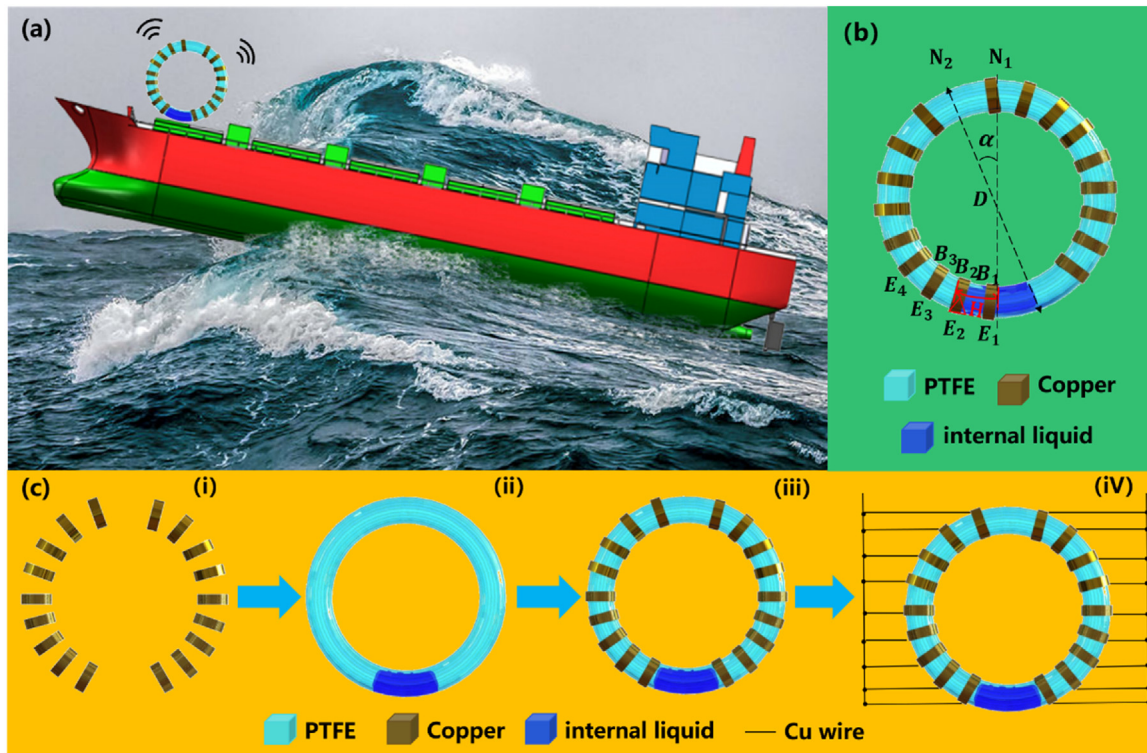


**Fig. 1.** Schematic design of the TENG tilt sensor. (a) schematic diagram of TENG tilt sensor applied to ship attitude sensing; (b) structure and principle of the TENG tilt sensor; (c) the fabrication process of TENG tilt sensor.

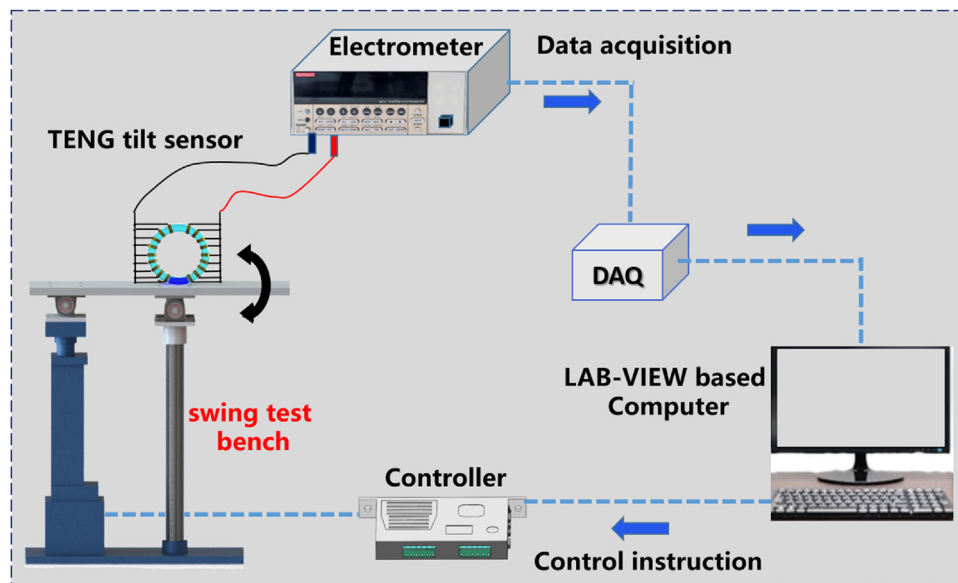


**Fig. 2.** TENG tilt sensor experimental apparatus.

trode position, causing the surrounding potential to increase, which in turn forms an electron transfer in the external circuit.

The PTFE always has a fixed amount of negative charges on its surface since PTFE material is electret. The transferred charge is primarily caused by electron transfer, and ion transfer is a minority effect according to the results of Nie et al. [37]. As the concentration of ions in the water increases, ions accumulate on the liquid-solid interface to create a screen effect, thereby reducing electron transfer. Furthermore, there is an obvious charge transfer between oil and PTFE that proves that the transferred charge can be generated without ions. This further illustrates the existence of electron

transfer in liquid-solid contact-electrification. When the internal liquid contacts the surface of the PTFE tube, there are only traces of hydrogen ions and hydroxide ions in pure water due to the electron transfer dominates the generation of contact electrification charges [38]. Positive charges in pure water are transferred to get close to the PTFE surface, and some hydrogen ions and hydroxide ions are also adsorbed on the PTFE surface, as shown in Fig. 3c. Electron transfer is a dominating effect of this liquid-solid electrification process. As ion concentration increases, the ion adsorption on the PTFE hinders electron transfer and results in the suppression of the transferred to charge amount. Ions can interfere with the process of

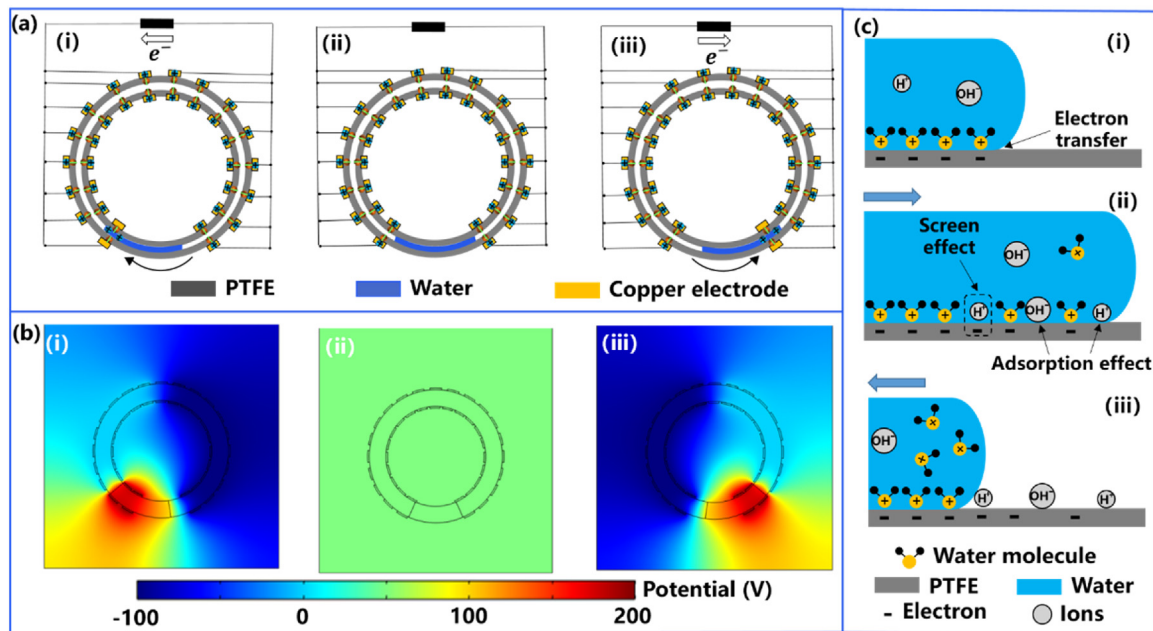


**Fig. 3.** Working principle of the TENG tilt sensor. (a) Schematic diagram of charge distribution of TENG tilt sensor. (b) Finite-element simulation of the potential distribution of the TENG tilt sensor under different tilt status. (c) Schematic diagram of the mechanism of contact electrification between water and PTFE material.

electron transfer by the screening effect. Some ions can be adsorbed on the PTFE surface due to electrostatic force. Electron transfer and hydrogen ion adsorption occur simultaneously, but a high concentration of hydrogen ions is adsorbed on the surface of the PTFE to suppress electron transfer between the water molecules and the PTFE.

The effect of pure water, tap water, salt solution on the TENG tilt sensor output signal is studied as depicted in Fig. 4. A swing test bench, the tilting angle of which covers  $-20$  to  $20$  degrees is used to simulate the swing motion of the TENG tilt sensor on board as shown in Fig. 4a. It is interesting to find that the peak voltage decreases dramatically as using NaCl solution with the salinity  $5 \text{ mg mL}^{-1}$  as depicted in Fig. 4b. Similar results are found in the tested current and transferred charge as shown in Fig. 4c and d. The ions in the liquid lead to the rapid reduction of the output signal of TENG tilt sensor. A larger output signal is beneficial to improve the sensitivity of the sensor. Therefore, pure water is adopted as the internal fluid of TENG tilt sensor for the current work. The ship's attitude change is a slow process under normal circumstances, and the mass of the liquid column in the tube is  $5 \text{ g}$ . Therefore, the inertial of the liquid in the tube is very small, and the impact on the sensor is negligible.

The relationship between the tilt angle and the internal liquid column conversion is shown in Fig. 1b, the diameter of the annular tube is defined as  $D$ , the stroke of the one-sided liquid column is  $\Delta H$ . Thus, the tilt angle  $\alpha$  can be obtained approximately by the following relations:

$$\alpha = 360\Delta H/\pi D\# \quad (2)$$

As long as the position of the electrode contacted with the internal liquid column is determined when it is tilted,  $\Delta H$  can be determined, and then the tilt angle can be obtained. When the internal fluid flows from  $E_1$  to  $E_3$  as shown in Fig. 5a and b, and its output voltage signal is shown in Fig. 5c and d. The green part shows the signal that the internal liquid flowing through the electrode when the TENG tilts to the left. The grey portion refers to the signal at which the internal liquid flowing through the electrode when the

TENG returns to the original position. The transferred charge has an opposite trend to the open circuit voltage according to the theory of triboelectric nanogenerator, but has almost the same signal characteristics as the signal slope at the electrode is larger compared to the blank position, as shown in Fig. 5e and f. The change of open circuit voltage and transferred charge has the same tendency for different width of the electrode. When the internal fluid increases from the  $E_1$  to  $E_3$ , the treated signal ( $dV_{OC}/dt$ ) of the TENG tilt sensor are shown in Fig. 5g and h. By reducing the electrode width, more peak signals can be detected in the same time interval, which is beneficial to improve the sensitivity of the TENG tilt sensor. Fig. 5h shows that three peak signals can be found in  $1 \text{ s}$ , which is verified that the TENG tilt sensor with a narrow electrode has higher sensitivity. In addition, it can be concluded that the real-time tilt angle  $\alpha$  can be obtained from the  $\Delta H$  value at different points of time. Experimental results show that the slope of the  $V_{OC}$  and  $Q_{SC}$  increases, while the peak value of the  $I_{SC}$  and  $dV_{OC}/dt$  occurs when the liquid column reaches the electrode position of the TENG tilt sensor. When the liquid column reaches the gap position between the electrodes, the slope of the  $V_{OC}$  and  $Q_{SC}$  is smaller than that generated by the liquid column flowing through the electrodes. Therefore, the number of peaks of the  $dV_{OC}/dt$  curve can be used to determine the position of the liquid column in the annular tube, and further to calculate the  $\Delta H$ . The tilt angle can be calculated by Eq. (2). The diameter ( $D$ ) of the annular is  $200 \text{ mm}$ . When the electrode width is  $2 \text{ mm}$ , the calculation error is about  $1.72^\circ$  according to Eq. (2) i.e.  $\alpha \pm 1.72^\circ$ . Positive and negative of the peak value can be used to determine the movement direction of the liquid column or the tilt direction. Similar results can be found when the internal liquid column flows through position  $B_3$  for different electrode width of the TENG tilt sensor as shown in Fig. S1. To improve the resolution of the sensor and the convenience of processing, a  $2 \text{ mm}$  electrode and a  $200 \text{ mm}$  diameter of the PTFE annular are used to fabricate the TENG tilt sensor.

The TENG can be treated as an ideal voltage source and an internal capacitor connected in series. For the TENG tilt sensor with multiple electrodes, the open circuit voltage  $V_{OC}$  gradually

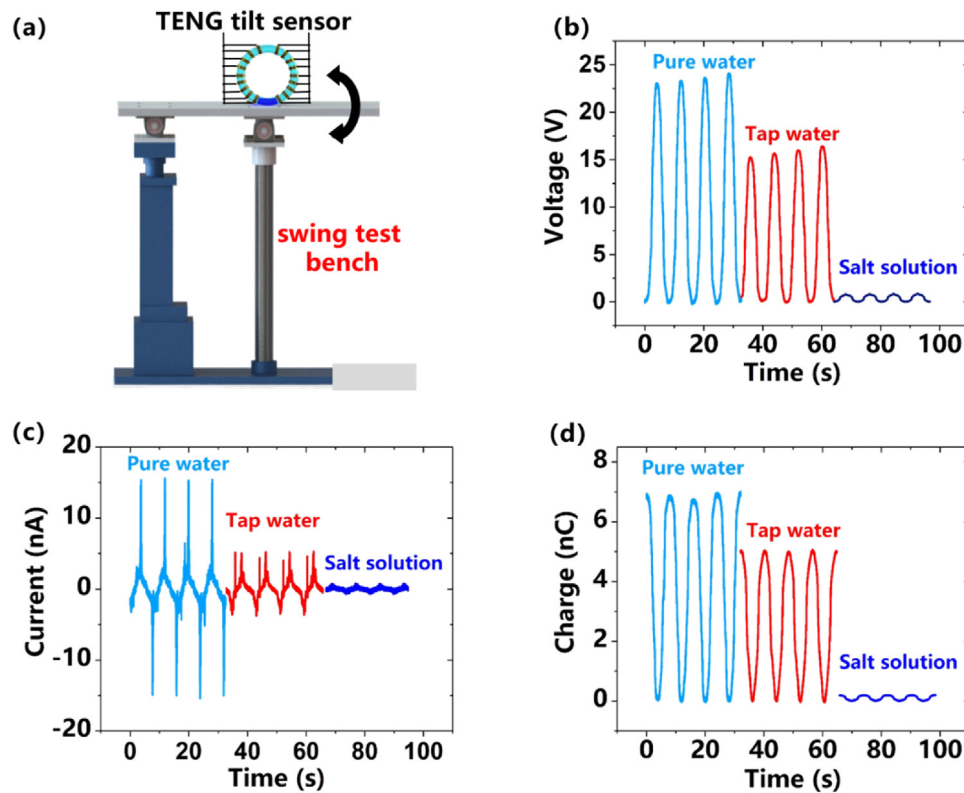


**Fig. 4.** The output performance of the TENG tilt sensor. (a) schematic of the experimental apparatus of the TENG tilt sensor; (b) open circuit voltage; (c) short circuit current; (d) transferred charge of the TENG tilt sensor with different type of liquid in it.

increases when the internal liquid flows from the bottom to another electrode, the  $V_{OC}$  can be determined as follows,

$$V_{OC} = V_{OCc} + V_{OCb} = \sum_i V_{OCc}^i + \sum_j V_{OCb}^j \quad (3)$$

where  $V_{OC}$  is the open circuit voltage,  $V_{OCc}$  is the induced voltage for internal fluid flowing over the  $i$  th bottom electrode region, and  $V_{OCb}$  is the induced voltage for internal fluid flowing over the  $j$  th blank region between a pair of neighboring bottom electrodes.

The performance of the TENG tilt sensor is further investigated when the internal fluid suddenly stops at a specific position. By controlling the start and stop of the swing test bench, the internal liquid passes through the electrode and is stationary for 2 s in the electrode blank area, its output signal is shown in Fig. S2. It can be found that when the internal liquid passes through the electrode,  $V_{OC}$  and  $Q_{SC}$  rise and fall obviously according to Eq. (3), and the peak value of the  $I_{SC}$  and  $dV_{OC}/dt$  occurs. When the internal liquid retains in the electrode gap,  $V_{OC}$  and  $Q_{SC}$  keep constant, the value of  $I_{SC}$  is zero, and the  $dV_{OC}/dt$  value is nearly constant zero, which can be used as a reference for tilting status at rest.

### 3.2. Application and outlook of the TENG tilt sensor

The application of TENG tilt sensor for ship attitude sensing is shown in Fig. 6a. The TENG tilt sensor is installed vertically in the ship model and the center is on the longitudinal section of the ship model. The real-time ship tilt angle can be reflected by a voltage signal as shown in Fig. 6b. Four electrodes and three electrode gaps are contacted with the internal liquid column. Fourteen feature points can be obtained during the rolling of the ship, and the tilt angles of the fourteen feature points are calculated separately by Eq. (3). The real-time ship tilt angle obtained by the TENG tilt sensor and a commercial sensor are compared, and they agree well as depicted

in Fig. 6c. The model of the commercial tilt sensor is WIT BWT901CL. The device output voltage is consistent in 5 days as shown in Fig. 6d, implying that the device is durable. A tilting monitoring system will be developed for indicating the real-time ship attitude. When the internal fluid flows through an electrode, the LED for indicating the corresponding angle is lit, which can be used as a tilt alarm system in many areas. When the inclination of the ship exceeds the dangerous value, the visualization system can trigger an alarm device to notify the crew to adjust the attitude of the ship or abandon the ship for life-saving. In addition, the annular closed structure makes the internal liquid isolated from the external environment, the performance of the sensor cannot be affected by environmental factors such as temperature and humidity, which makes it have the characteristics of robust and longer-lasting.

## 4. Conclusion

In summary, a robust and self-powered tilt sensor based on annular liquid-solid interfacing triboelectric nanogenerator (TENG), which has the outstanding characteristics of self-powered and robust has been proposed and systematically studied, and it can be used to monitor the real-time tilt information of ships, ocean platforms and other special ocean equipment. In particular, self-powered and robust characteristics are the advantages of the TENG tilt sensor. By conducting performance test experiments, a structure-optimized TENG tilt sensor with an electrode width of 2 mm and pure water as the internal fluid has been developed. The  $V_{OC}$  and  $Q_{SC}$  are found increasing with the growth of the tilt angle. Meanwhile, the peak value of  $dV_{OC}/dt$  and  $I_{SC}$  occurs when the liquid column flows through the electrode attached on the tube. Significantly, the positive and negative of the peak value of  $dV_{OC}/dt$  can be used to determine the tilt direction of the ship. Moreover, the TENG tilt sensor is sensitive to low-frequency and low-amplitude

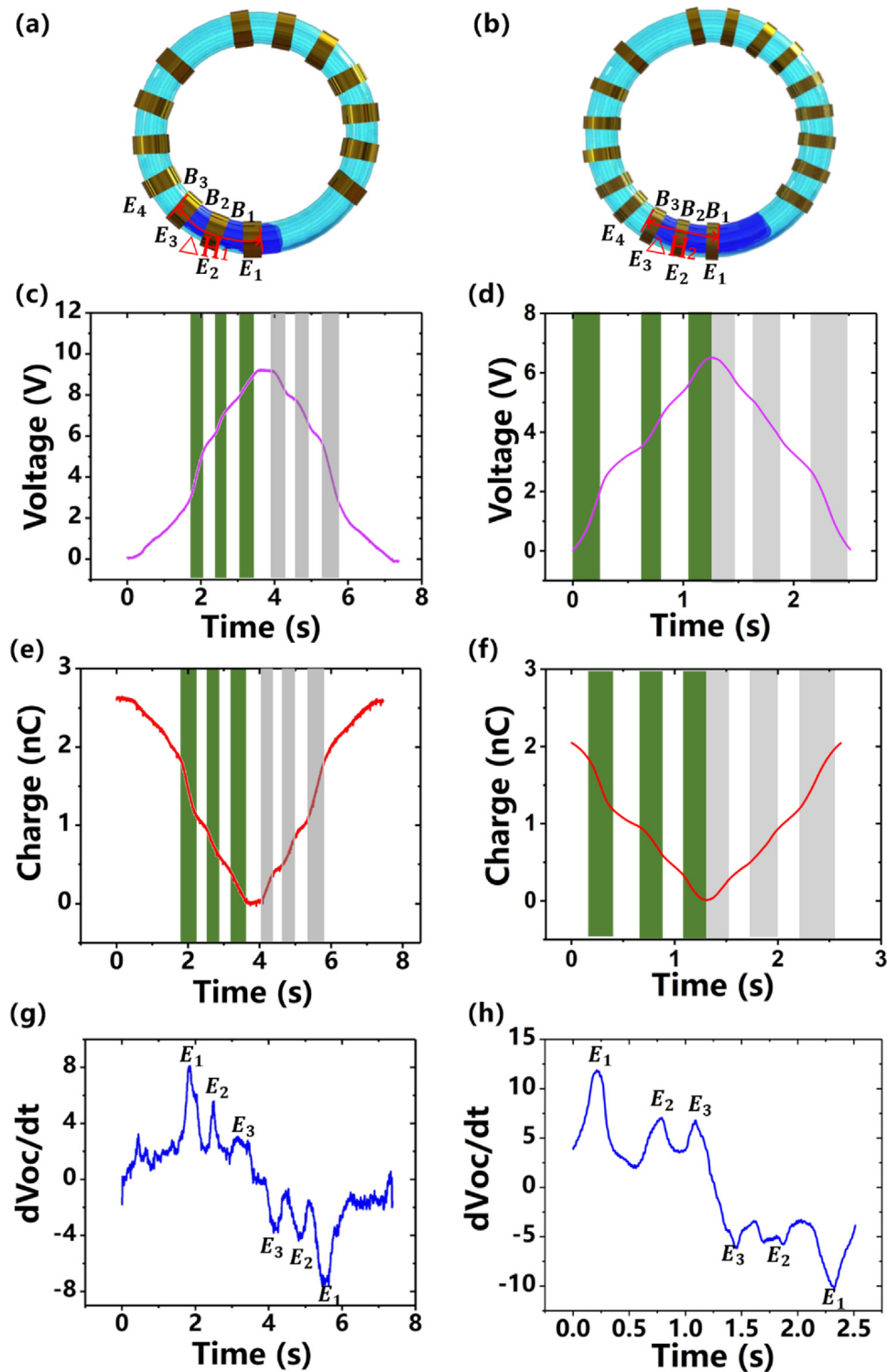


**Fig. 5.** The output characteristics of the TENG tilt sensor with different electrode width. Schematic diagram of TENG tilt sensor (a) with the electrode width of 5 mm; (b) with the electrode width of 2 mm; output voltage signal when the internal fluid increases from  $E_1$  to  $E_3$  (c) with the electrode width of 5 mm; (d) with the electrode width of 2 mm; output transferred charge ( $Q_{sc}$ ) signal when the internal fluid increases from  $E_1$  to  $E_3$  (e) with the electrode width of 5 mm; (f) with the electrode width of 2 mm; the  $dV_{oc}/dt$  of the TENG tilt sensor when the internal fluid increases from  $E_1$  to  $E_3$  (g) with the electrode width of 5 mm; (h) with the electrode width of 2 mm.

inclination. More importantly, the TENG tilt sensor can hardly be affected by the external environment due to its specific structure, which verified the robustness of TENG tilt sensor. This study further expands the application of self-powered sensors by proposing a TENG tilt sensor and takes another important step in monitoring the tilt information of ship.

#### CRediT authorship contribution statement

**Song Wang:** Conceptualization, Methodology, Software. **Yan Wang:** Data curation, Writing - original draft. **Dehua Liu:** Formal analysis, Data curation. **Ziyi Zhang:** Validation. **Wenxiang Li:** Software. **Changxin Liu:** Software, Validation. **Taili Du:** Validation.

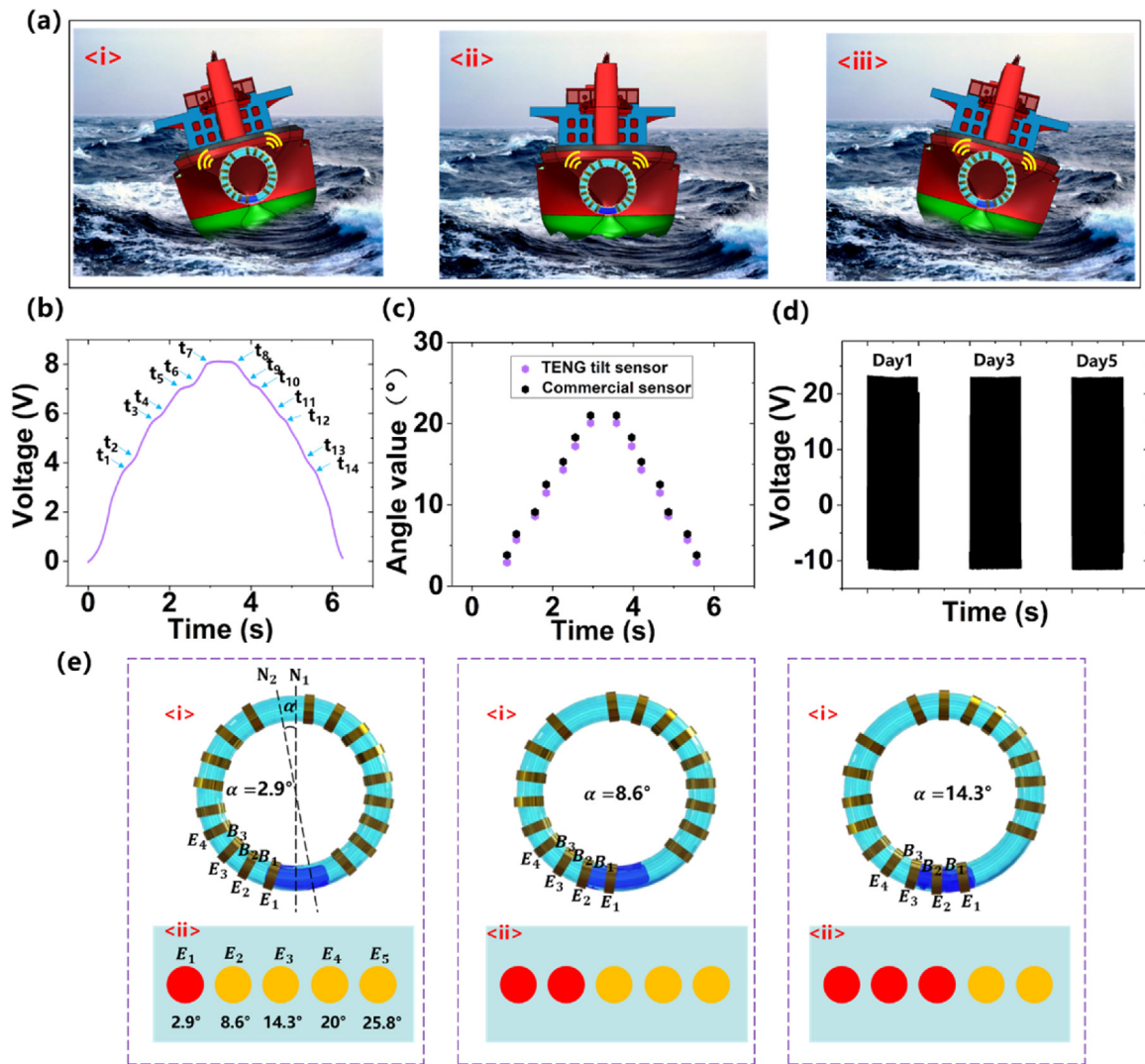


**Fig. 6.** The application and outlook of the TENG tilt sensor for ship attitude sensing. (a) schematic diagram of TENG tilt sensor for monitoring the heel of a ship; (b) the TENG tilt sensor output signal diagram in the ship model experiment; (c) comparison of the TENG tilt sensor and a commercial sensor; (d) the durability of the sensor tested for 5 days; (e) schematic diagram and display interface for indicating the real-time tilting angle.

**Xiu Xiao:** Supervision. **Liguo Song:** Investigation. **Hongchen Pang:** Writing - review & editing. **Minyi Xu:** Supervision, Writing - review & editing.

**Declaration of Competing Interest**

The authors report no declarations of interest.

**Acknowledgments**

The authors are grateful for the joint support from the National Natural Science Foundation of China (Grant Nos. 51879022, 51979045, 51906029), the Chinese Government Scholarship (CSC No. 202006570022), the Fundamental Research Funds for the Central Universities, China (Grant No. 3132019330), and Projects for Dalian Youth Star of Science and Technology (Grant No. 2018RQ12).

**Appendix A. Supplementary data**

Supplementary material related to this article can be found, in the online version, at doi:<https://doi.org/10.1016/j.sna.2020.112459>.

**References**

- [1] B.-G. Paik, S.-R. Cho, B.-J. Park, D. Lee, B.-D. Bae, J.-H. Yun, J. Mar. Sci. Tech-Japan 14 (2009) 115–126.
- [2] B.G. Paik, S.R. Cho, B.J. Park, D. Lee, J.H. Yun, B.D. Bae, in: International Conference on Embedded & Ubiquitous Computing, 2007, pp. 113–122.
- [3] USNAVY, Interface Standard for Shipboard Systems Section 301a Ship Motion and Attitude, 1986.
- [4] X. Peng, X. Zhao, L. Xu, in: International Symposium on Systems & Control in Aerospace & Astronautics, 2006.
- [5] R. Olaru, D.D. Dragoi, Sens. Actuators A-Phys. 120 (2005) 424–428.
- [6] B.O. Guan, H.-Y. Tam, S.-Y. Liu, IEEE Photonics Technol. Lett. 16 (2004) 224–226.
- [7] J.-H. Wu, K.-Y. Horng, S.-L. Lin, R.-S. Chang, Meas. Sci. Technol. 17 (2006) N9–N12.
- [8] X. Zou, P. Thiruvengathanathan, A. Seshia, in: IEEE International Frequency Control Symposium, 2012.
- [9] S.L. Zhang, M. Xu, C. Zhang, Y.-C. Wang, H. Zou, X. He, Z. Wang, Z.L. Wang, Nano Energy 48 (2018) 421–429.
- [10] Y. Wang, J. Wang, X. Xiao, S. Wang, T.K. Phan, J. Dong, J. Mi, X. Pan, H. Wang, M. Xu, Nano Energy 73 (2020) 104736.
- [11] M. Xu, T. Zhao, C. Wang, S.L. Zhang, Z. Li, X. Pan, Z.L. Wang, ACS Nano 13 (2019) 1932–1939.
- [12] H. Zhang, H. Wang, J. Zhang, Z. Zhang, Y. Yu, J. Luo, S. Dong, Sens. Actuators A-Phys. 302 (2020), 111806.
- [13] X. Xiao, X. Zhang, S. Wang, H. Ouyang, P. Chen, L. Song, H. Yuan, Y. Ji, P. Wang, Z. Li, M. Xu, Z.L. Wang, Adv. Energy Mater. 9 (2019), 1902460.
- [14] H. Zhao, X. Xiao, P. Xu, T. Zhao, L. Song, X. Pan, J. Mi, M. Xu, Z.L. Wang, Adv. Energy Mater. 9 (2019), 1902824.

- [15] X. Zhang, M. Yu, Z. Ma, H. Ouyang, Y. Zou, S.L. Zhang, H. Niu, X. Pan, M. Xu, Z. Li, Z.L. Wang, *Adv. Funct. Mater.* 29 (2019), 1900327.
- [16] M. Xu, Y. Wang, S.L. Zhang, W. Ding, J. Cheng, X. He, P. Zhang, Z. Wang, X. Pan, Z.L. Wang, *Extrem. Mech. Lett.* 15 (2017) 122–129.
- [17] S.L. Zhang, M. Xu, C. Zhang, Y. Wang, H. Zou, X. He, Z. Wang, Z.L. Wang, *Nano Energy* 48 (2018) 421–429.
- [18] Z.L. Wang, *Mater. Today* 20 (2017) 74–82.
- [19] M. Xu, S. Wang, S.L. Zhang, W. Ding, K.T. Phan, C. Wang, Z. Li, X. Pan, Z.L. Wang, *Nano Energy* 57 (2019) 574–580.
- [20] X. Liu, A. Yu, A. Qin, J. Zhai, *Int. J. Adv. Mater. Technol.* 4 (2019), 1900608.
- [21] J. Yin, X. Li, J. Yu, Z. Zhang, J. Zhou, W. Guo, *Nat. Nanotechnol.* 9 (2014) 378.
- [22] J. Yin, Z. Zhang, X. Li, J. Yu, J. Zhou, Y. Chen, W. Guo, *Nat. Commun.* 5 (2014) 3582.
- [23] Z. Lin, G. Cheng, S. Lee, K.C. Pradel, Z.L. Wang, *Adv. Mater.* 26 (2014) 4690–4696.
- [24] X. Zhang, Y. Zheng, D. Wang, F. Zhou, *Nano Energy* 40 (2017) 95–106.
- [25] L. Pan, J. Wang, P. Wang, R. Gao, Y.-C. Wang, X. Zhang, J.-J. Zou, Z.L. Wang, *Nano Res.* 11 (2018) 4062–4073.
- [26] Y. Su, G. Xie, S. Wang, H. Tai, Q. Zhang, H. Du, H. Zhang, X. Du, Y. Jiang, *Sens. Actuators B-Chem.* 251 (2017) 144–152.
- [27] B. Zhang, L. Zhang, W. Deng, L. Jin, F. Chun, H. Pan, B. Gu, H. Zhang, Z. Lv, W. Yang, Z.L. Wang, *ACS Nano* 11 (2017) 7440–7446.
- [28] M. Xu, S. Wang, S.L. Zhang, W. Ding, P.T. Kien, C. Wang, Z. Li, X. Pan, Z.L. Wang, *Nano Energy* 57 (2019) 574–580.
- [29] T.K. Phan, S. Wang, Y. Wang, H. Wang, X. Xiao, X. Pan, M. Xu, J. Mi, *Sensors (Basel)* 20 (2020) 729.
- [30] M. Xu, P. Wang, Y. Wang, S.L. Zhang, A.C. Wang, C. Zhang, Z. Wang, X. Pan, Z.L. Wang, *Adv. Energy Mater.* 8 (2018), 1702432.
- [31] Z. Wu, W. Ding, Y. Dai, K. Dong, C. Wu, L. Zhang, Z. Lin, J. Cheng, Z.L. Wang, *ACS Nano* 12 (2018) 5726–5733.
- [32] H. Guo, J. Chen, L. Tian, Q. Leng, Y. Xi, C. Hu, *ACS Appl. Mater. Interfaces* 6 (2014) 17184–17189.
- [33] J. Sun, A. Yang, C. Zhao, F. Liua, Z. Li, *Sci. Bull.* 64 (2019) 1336–1347.
- [34] X. Cui, C. Zhang, W. Liu, Y. Zhang, J. Zhang, X. Li, L. Geng, X. Wang, *Sens. Actuators A-Phys.* 280 (2018) 326–331.
- [35] Y. Su, G. Xie, X. Tao, H. Zhang, Z. Ye, Q. Jing, H. Tai, X. Du, Y. Jiang, *J. Phys. D Appl. Phys.* 49 (2016), 215601.
- [36] S. Niu, Y. Liu, S. Wang, L. Lin, Y.S. Zhou, Y. Hu, Z.L. Wang, *Adv. Mater.* 25 (2013) 6184–6193.
- [37] J. Nie, Z. Ren, L. Xu, S. Lin, F. Zhan, X. Chen, Z.L. Wang, *Adv. Mater.* 32 (2020), 1905696.
- [38] J. Nie, Z. Ren, L. Xu, S. Lin, Z.L. Wang, *Adv. Mater.* 32 (2020), 1905696.

## Biographies



**Song Wang** received his master degree in Dalian Maritime University, China. His research focuses on liquid-solid interfacing triboelectric nanogenerator for energy harvesting and self-powered sensors.



**Yan Wang** is currently pursuing his doctor degree in Dalian Maritime University, China. His current research interests include flow-induced vibration, blue energy, self-powered systems and triboelectric nanogenerators.



**Dehua Liu** is currently pursuing the master's degree in Dalian Maritime University, China. His current research direction is the self-powered system of life-saving equipment based on triboelectric nanogenerators.



**Ziyi Zhang** is currently pursuing his master degree in Dalian Maritime University, China. His current research interests in liquid-solid TENG, blue energy and self-powered systems.



**Wenxiang Li** received the B.E degree in Marine Engineering from Dalian Maritime University, Dalian, China. He is currently pursuing the master degree in Marine Engineering College, Dalian Maritime University, Dalian, China. His current research interests include design and control of underwater robots and triboelectric nanogenerator.



**Changxin Liu** received his Ph.D. degree from in Dalian University of technology in 2013. His current research is mainly focused on the semiconductor thermoelectric power generation, ship energy saving, triboelectric nanogenerators and composite energy harvesting field.



**Taili Du** received his B.S. and M. S. from Dalian Maritime University in China in 2008 and 2010. Since 2010, he is with Dalian Maritime University where he is currently an Associate Professor. Currently, he is as a doctoral candidate in Marine Engineering College, Dalian Maritime University. His current research work focus on intelligent equipment performance monitoring and self-powered sensor based on Triboelectric Nanogenerator.





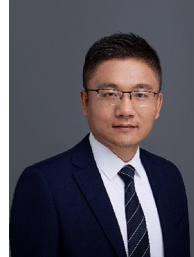
**Dr. Xiu Xiao** received her Ph.D. degree from Tsinghua University in 2017. During 2014–2016, she was a visiting scholar in Purdue University. Now she is an associate professor in Marine engineering College, Dalian Maritime University. Her research interests include new energy harvesting technology and energy saving.



**Pang Hongchen** is currently an Associate Professor in School of Mechanical and Power Engineering, Guangdong Ocean University. His current research is mainly focused on ocean energy technology.



**Dr. Liguang Song** received his Ph.D. degree from Dalian Maritime University in 2020. He is a second engineer officer of ships powered by main propulsion machinery of 3000 kW propulsion power or more. Now he is an Associate Professor in the Marine Engineering College, Dalian Maritime University. His current research is mainly focused on the areas of blue energy, ship exhaust pollution control, triboelectric nanogenerators and its practical applications in smart ship and ocean.



**Dr. Minyi Xu** received his Ph.D. degree from Peking University in 2012. During 2016–2017, he joined Professor Zhong Lin Wang' group at Georgia Institute of Technology. Now he is a Professor in the Marine Engineering College, Dalian Maritime University. His current research is mainly focused on the areas of blue energy, self-powered systems, triboelectric nanogenerators and its practical applications in smart ship and ocean.